transformations," J. Stat. Phys. **19**, 25–52 (1978).
[2]H. G. Schuster, "Deterministic chaos," Physik-Verlag GmbH, Weinheim (1984).
[3]See, e.g., A. J. Diefenderfer, *Principles of Electronic Instrumentation* (W. B. Saunders, Philadelphia, 1972), p. 284.
[4]B. van der Pol, "Forced oscillations in a circuit with nonlinear resistance," Phil. Mag. **2**, 21–27 (1926); **3**, 65–80 (1927).
[5]E. Atlee Jackson, *Perspectives of Nonlinear Dynamics* (Cambridge U. P., Cambridge, 1989).
[6]This feature is shown by e.g., the Kikusui COS 6100, the Trio CS 1830, and the Philips PM 3070 oscilloscopes.
[7]The redefinition of F is just convenient for the simulations. The real significance of a physical change in sign of the diode response (corresponding to a polarity change of the diode) is just to mirror the signals on the oscilloscope.
[8]Preben Alstrøm, Bo Christiansen, and Mogens T. Levinsen, "Routes to chaos in a modulated relaxation oscillator," Phys. Rev. **A42**, 1891–1900 (1990).
[9]M. H. Jensen, P. Bak, and T. Bohr, "Complete devil's staircase, fractal dimension and universality of mode-locking structures," Phys. Rev. Lett. **50**, 1637–1639 (1983).
[10]Since the system is nonautonomous (i.e., directly dependent on time), the map is generated here by strobing (measuring once per revolution) with the external drive frequency. This is done by connecting the external signal to the external clock input of the waveform analyzer.
[11]Since the maximum response occurs when the trace passes most closely to the position of the diode, a phase shift takes place between the original signal and the light-induced response. A local maximum may in fact occur twice in the movement back and forth across the screen. Hence, the second harmonic may be observed. This should not be confused with the possible parametric excitation of a second harmonic, see, e.g., M. T. Levinsen, "Even and odd subharmonic frequencies and chaos in Josephson junctions; Impact on parametric amplifiers," J. Appl. Phys. **53**, 4294–4299 (1982), for a discussion of this effect.
[12]P. S. Lindsay, "Period doubling and chaotic behavior in a driven anharmonic oscillator," Phys Rev. Lett. **47**, 1349–1352 (1981); see also Ref. 5, Fig. 5.144, p. 357.
[13]Claude Baesens, "Slow sweep through a period-doubling cascade: Delayed bifurcations and renormalization," Physica **D53**, 319–375 (1992).

Microwave experiments on electromagnetic evanescent waves and tunneling effect

Francisco Albiol, Sergio Navas, and Miguel V. Andres
Departamento de Física Aplicada, Universidad de Valencia, Dr. Moliner 50, 46100 Burjassot (Valencia), Spain

(Received 2 January 1992; accepted 26 July 1992)

A set of experiments is described to measure the decay of electromagnetic evanescent waves and the tunneling effect through an airgap. The experiments are performed using microwaves and have been designed to be carried out by third year students of physics. The proposed experimental setup can be regarded as a quantum mechanical simulator for the one-dimensional motion of a particle.

I. INTRODUCTION

The total internal-reflection of electromagnetic waves is a phenomenon that always causes a particular interest among students. This phenomenon leads to the concepts of evanescent wave and tunneling effect which are used in modern physics in different fields and applications, such as integrated optics,[1] metrology,[2] quantum mechanics,[3] superconductivity,[4] scanning tunneling microscope,[5] etc.

We present here a set of microwave experiments that have been designed for third year physics students. The aim of these experiments is to measure the decay of electromagnetic evanescent waves and the transmission through an airgap based on electromagnetic tunneling effect. The use of microwaves, instead of, for example, light,[6] simplifies the mechanical requirements for stability and position measurements. Furthermore, the microwave components required for our experiments are readily available from standard manufacturers of equipment for educational physics laboratories. Our experimental arrangements and procedures have several advantages over other previous microwave experiments,[7] such as the direct measurement of the exponential decay of the evanescent waves, the use of dielectric pellets to make a prism of variable angle, and the use of modern microwave devices.

We should mention that one advantage of using visible light to investigate the electromagnetic tunneling is that it permits the detection of individual photons.[8] The individual photon tunneling cannot be demonstrated using microwaves. However, the instruments required for such an optical experiment are not usually available in an undergraduate physics laboratory.

We have found it interesting to include a discussion of the equivalence of these electromagnetic phenomena and the quantum mechanical description of one-dimensional motion. We show the possibility of regarding our experimental arrangement as a quantum mechanical simulator. Eventually, our experimental setup could be used to test the numerical calculations described by Leming and Van Smith[9] to study the quantum barrier penetration in one dimension.

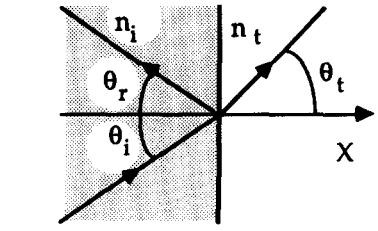

(a)

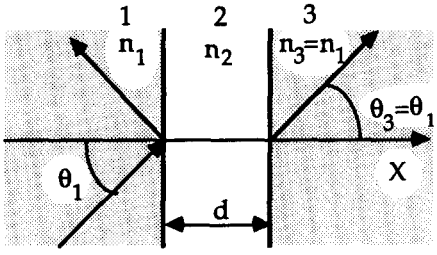

(b)

Fig. 1. (a) Reflection and refraction at a plane boundary. (b) Tunneling through a dielectric layer of thickness d.

II. THEORY

A. Total reflection: Generation of evanescent waves

The incidence of a plane wave onto a plane boundary between two dielectric media of refractive index n_i and n_t [Fig. 1(a)] is described by the expressions:

$$\theta_i=\theta_r, \qquad n_i \sin\theta_i=n_t \sin\theta_t. \tag{1}$$

The phenomenon of total reflection occurs when $n_i>n_t$ and the angle of incidence θ_i is greater than a critical angle θ_c defined by

$$\sin\theta_c=n_t/n_i. \tag{2}$$

When total reflection takes place, the angle of refraction θ_t has a complex value which gives rise to a transmitted plane wave[10] with a particular dependence on x:

$$\mathbf{E}=\mathbf{E}_0 \exp(jk_x x)=\mathbf{E}_0 \exp(-hx), \tag{3}$$

where k_x is the x component of the wave-number vector and h is defined by $k_x=jh$ ($j\equiv\sqrt{-1}$):

$$k_x=(2\pi/\lambda)n_t\cos\theta_t, \qquad h=\frac{2\pi}{\lambda}n_t\left[\left(\frac{\sin\theta_i}{\sin\theta_c}\right)^2-1\right]^{1/2}. \tag{4}$$

Equation (3) defines an evanescent wave with a spatial decay coefficient h. Such a wave gives no net power flow in the x direction and, therefore, total reflection takes place. The decay coefficient h of an evanescent wave and its dependence on θ_i will be investigated in our first experiment.

B. Electromagnetic tunneling effect

We shall assume through the rest of the paper that the incident wave is TE polarized. However, similar expressions can be derived for TM incidence.[7]

Figure 1(b) gives a diagram of a system where two dielectric media are separated by a second medium of finite thickness d. If we assume that $n_1=n_3>n_2$ and that the angle of incidence θ_1 is greater than the critical angle for total reflection, then we might expect no power transmitted through medium 2 into medium 3. However, the exponential tail of an evanescent wave is able to couple some power between two media provided their separation is finite. Indeed, if we work out the fields in medium 3 we find that the relative power transmission[10] T from medium 1 to medium 3 is given by

$$T=\frac{1}{1+\{[(k_1^2-k_2^2)/2k_1k_2]\sin(k_2d)\}^2}, \tag{5}$$

where

$$k_1=(2\pi/\lambda)n_1\cos\theta_1, \qquad k_2=(2\pi/\lambda)n_2\cos\theta_2, \tag{6}$$

in our case θ_2 will be complex, since we are assuming $\theta_1>\theta_c$, and therefore cannot be plotted in Fig. 1(b).

The transmission T can be rewritten, taking $\theta_1=\theta_i>\theta_c$, $n_1=n$, $n_2=1$, and $k_2=jh$, as

$$T=\frac{1}{1+[Q\sinh(hd)]^2}, \qquad Q=\frac{k_1^2+h^2}{2k_1h}=\frac{n^2-1}{2n\cos\theta_i(n^2\sin^2\theta_i-1)^{1/2}}. \tag{7}$$

The fact that the power coupling is determined by an evanescent wave leads to a critical dependence on h and d. Such a coupling is referred to as a frustrated total reflection or a tunneling effect. Our second experiment will consist of measuring the tunneling through an airgap as a function of its thickness d.

C. Quantum mechanical analogy

Let us compare the one-dimensional Schrödinger equation

$$\frac{d^2\Psi(x)}{dx^2}=-\frac{p^2}{\hbar^2}\Psi(x), \tag{8}$$

with the one-dimensional wave equation for monochromatic electromagnetic radiation

$$\frac{d^2\xi(x)}{dx^2}=-k_x^2\xi(x), \tag{9}$$

where $\Psi(x)$ is the wave function of a particle of linear momentum p, mass m, total energy E, and potential energy $V(x)$, and $\xi(x)$ is any component of the electric or magnetic fields and k_x is the x component of the wave-number vector. Thus, the one-dimensional quantum mechanical motion and the propagation of a monochromatic electromagnetic wave satisfy identical equations, provided we establish the equivalence

$$k_x\leftrightarrow p/\hbar, \qquad k_x^2=\left(\frac{2\pi}{\lambda}n\cos\theta\right)^2\leftrightarrow\left(\frac{p}{\hbar}\right)^2=2m[E-V(x)]/\hbar^2. \tag{10}$$

Such an equivalence provides the basis for regarding the electromagnetic system as a quantum mechanical simula-

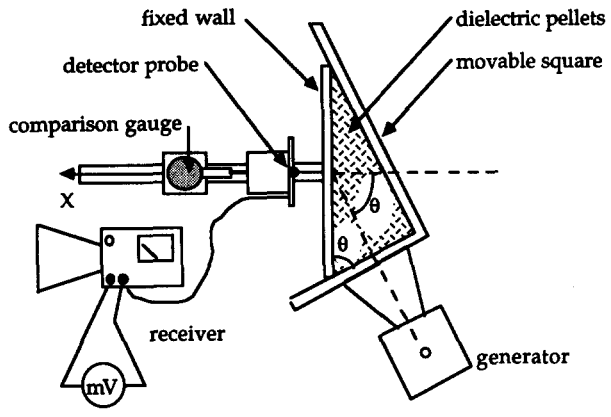

Fig. 2. Diagram of the experimental arrangement to generate microwave evanescent waves.

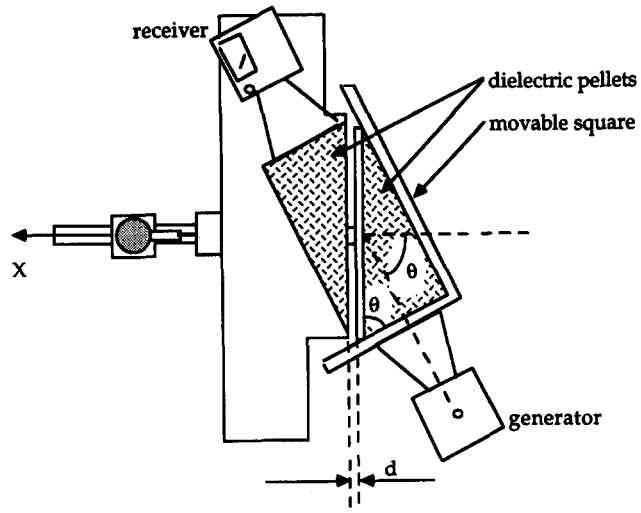

Fig. 3. Diagram of the experimental arrangement to measure the tunneling effect through an airgap.

tor.[3,6,8] In fact, the wave function $\Psi(x)$ for a particle incident upon an infinitely wide barrier of potential V_0, greater than its total energy E, exhibits an exponential tail penetrating the barrier

$$\Psi(x) \propto \exp\{-\{(2m/\hbar)[V(x)-E]\}^{1/2} x\} \qquad (11)$$

and the transmission through a potential barrier V_0 of thickness d is

$$T=\frac{1}{1+\{[(p_1^2-p_2^2)/2p_1p_2]\sin(p_2d/\hbar)\}^2}. \qquad (12)$$

Both, Eqs. (11) and (12), are identical to Eqs. (3) and (5) once the equivalence (10) is taken into account.

III. EXPERIMENTAL ARRANGEMENTS

A. Characteristics of evanescent waves

Figure 2 is a diagram of our experimental setup to generate evanescent waves and to measure their characteristics. The core of the system is a prism of variable angle, filled with metacrylate pellets. The lateral walls of the prism are metacrylate slabs of 1 cm thickness, one wall is fixed while the other two at right angles define a movable square. This square is held firmly against the fixed wall by four ball bearings mounted on springs. The angle can be adjusted within the interval [25°, 63°]. Alternatively, a set of prisms with fixed angles could be used, which would allow for the use of wax and other dielectric materials.[11]

The microwave generator, the detector probe, and the receiver with a built-in amplifier are all standard PASCO Scientific components for educational laboratories. The generator is a Gunn diode mounted in a 10.5 GHz resonant cavity ($\lambda=2.9$ cm) and a horn antenna, which provides 15 mW of linearly polarized radiation. The receiver includes a horn antenna, a diode mounted in a 10.5 GHz resonant cavity, an amplifier, a meter, and an output for an external meter. This receiver includes, as well, an input to fit a detector probe which consists of a diode with no horn nor resonant cavity. The detector probe was mounted on a bench, and a comparison mechanical dial gauge with 0.01 mm reading was used to measure the position of the probe along the x axis.

The experimental procedure for measuring the exponential decay of the evanescent waves consists of adjusting the angle θ (measured with a Bevel-protractor), placing the detector probe at $x=0$, adjusting the position of the generator horn against the prism wall to give the maximum signal at the detector and then measuring the detected signal as a function of x. The receiver horn and its built-in diode are not used in this experiment, since we use the external detector probe; therefore, some attention has to be paid to direct the receiver horn away from the microwave beam to prevent incorrect measurements. Alternatively, a standard dc-coupled amplifier could be used instead of the amplifier of the receiver. To improve the sensitivity of our system we used an external voltmeter connected to the amplifier output instead of the built-in meter.

The validity of the proposed experimental procedure depends on the correctness of the assumption that the perturbation of the evanescent wave by the detector probe is negligible. In fact, the detector probe has been designed by the manufacturer to measure the standing wave pattern in interferometric experiments, where again a non-negligible perturbation would destroy the pattern. This kind of detector probe cannot be imagined at optical wavelengths.

B. Tunneling effect

Figure 3 gives a diagram of the experimental setup used to measure the electromagnetic tunneling effect through an airgap of thickness d. Now, a platform has been mounted on the bench instead of the detector probe. This platform is used to support the microwave detector and a metacrylate prism of fixed walls (angles: 60°, 90°, and 30°) filled with metacrylate pellets. The angle of the variable prism has to be adjusted to 60° to match the other prism. The thickness of the airgap is measured with the comparison gauge as in the previous arrangement.

The experiment consists of measuring the transmission through the airgap as a function of its thickness d. Obviously, the maximum transmission will be obtained for $d=0$ when the beam goes directly from the generator to the receiver, this signal can be used to normalize the transmission.

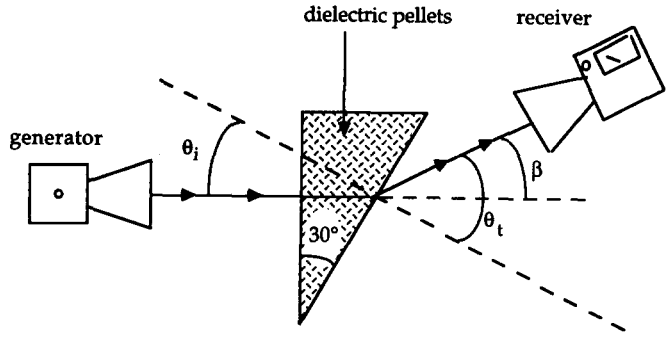

Fig. 4. Diagram of the experimental arrangement to measure the refractive index of the metacrylate pellets.

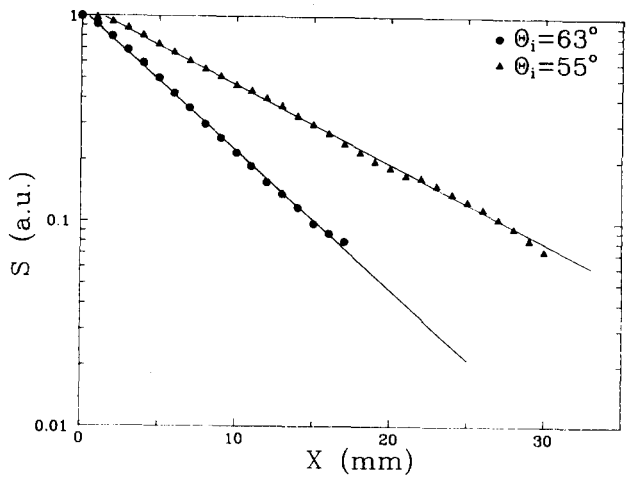

Fig. 5. Exponential decay of evanescent waves: detector probe signal S versus penetration depth x.

IV. EXPERIMENTAL RESULTS AND DISCUSSION

Before the experiments described in Secs. III A and B, three simple experiments were carried out to measure the refractive index of the metacrylate pellets at 10.5 GHz (i), and to test the linearity of the detector probe (ii) and the receiver (iii). The experiment (i) consisted of measuring the angle of refraction for an angle of incidence $\theta_i=30°$, using the prism of fixed walls used in Sec. III B. Figure 4 is a diagram of the experimental arrangement, where the receiver is mounted on a movable arm of a goniometer and the angle β is adjusted to give the maximum signal on the receiver built-in meter. The result was a refraction angle $\theta_t=39°\pm1°$, which gives $n=1.26\pm0.03$. This result determines the critical angle for total reflection, Eq. (2) $\theta_c=52.5°\pm1.8°$.

The other two experiments, (ii) and (iii), consisted of measuring the signal detected by the detector probe and the receiver as a function of the intensity of the incident wave. Since both are polarization sensitive, the method used to control the incident intensity was to rotate the emitter, scanning the interval [0°, 90°]. If α is the angle of rotation of the emitter, then the detector signal S will be determined by the component of the electric field $E_0\cos\alpha$. Plotting $\log(S)$ versus $\log(\cos\alpha)$ we can check the linearity of our detectors.[12] The signal of the detector probe exhibited a slope $m_p=1.74$, while the receiver exhibited a slope $m_r=1.51$. These results show that neither the detector probe nor the receiver measure the power or the electric field of the incident microwave, but an intermediate value. If we plan to carry out a quantitative checking of the theoretical equations derived in Sec. II, then it will be necessary to take into account these experimental calibrations.

Once the preliminary experiments have been performed, a first experiment was carried out, with the experimental arrangement of Sec. III A, measuring the detected signal S as a function of x for different angles θ_i, within the interval [55°, 63°]. Figure 5 shows the exponential decay for two different angles of incidence.

The results are satisfactory since they show the expected exponential dependence on x, Eq. (3). The slope of these plots can be used to calculate the decay coefficient h. Such a calculation requires taking into account the calibration of the detector probe

$$\ln(S/S_0)=m_p\ln(E/E_0)=-m_phx, \tag{13}$$

where S_0 and E_0 are the values of S and E at $x=0$.

We have worked out the h values for different angles of incidence θ_i. Figure 6 is a plot of h^2 versus $\sin^2\theta_i$. The bars plotted in this figure give the experimental error obtained after measuring repeatedly the exponential decay for the two angles $\theta_i=55°$ and $\theta_i=63°$. The origin of such error bars is not the decay measurements, since Fig. 5 shows an accurate exponential dependence on x, but the finite size of the microwave beam. Any small misalignment of the emitter horn generates a change on the measured decay. In fact, the equations derived in Sec. II do not apply for finite size beams, which require more detailed calculations.[13] Furthermore, a new interesting phenomenon appears when dealing with bounded beams, i.e., the Goos–Haenchen shift. This phenomenon can be demonstrated using the equipment described for our experiments.[14]

Figure 6 includes the theoretical curve, Eq. (4), taking $n_i=1.26$ and a best fitting of the same equation as a function of n_i, giving $n_i=1.23$. This result shows that the ap-

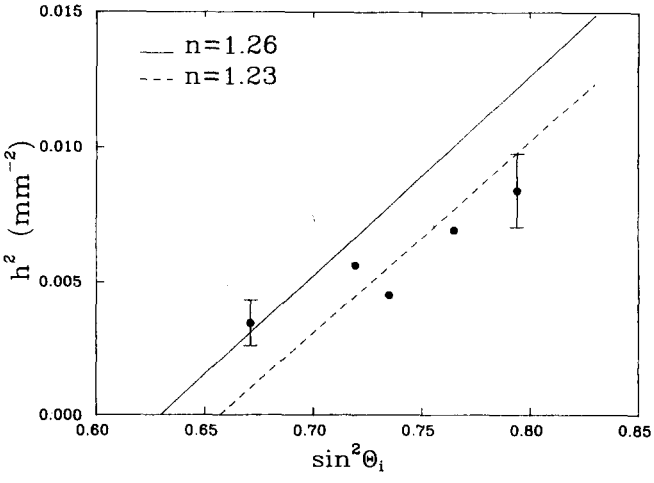

Fig. 6. Decay coefficient square h^2 as a function of the sine square of the angle on incidence $\sin^2\theta_i$. (●) Experimental points, (—) theoretical curve with $n=1.26$, (- -) best fit as a function of n.

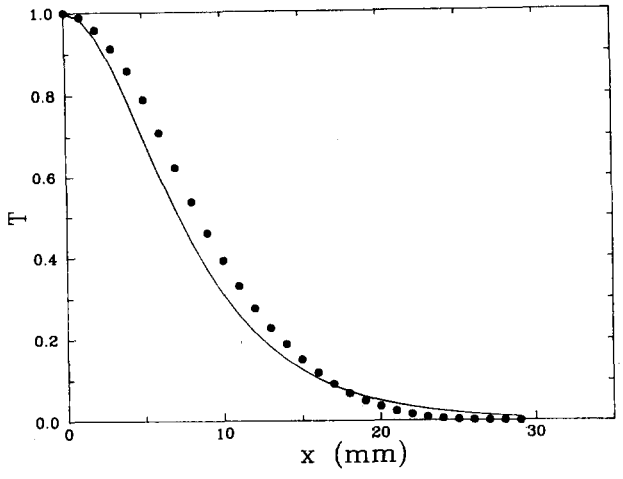

Fig. 7. Measured tunneling effect (•) and theoretical transmission for $n=1.26$ (—).

proximations assumed when we apply Eq. (4) are reasonably correct and that the experimental procedure is satisfactory.

The results obtained for the electromagnetic tunneling effect, using the experimental arrangement described in Sec. III B ($\theta_i=60°$), are given in Fig. 7. Taking into account the calibration of the receiver, $m_r=1.51$, we worked out T using the expression

$$\ln(T)=m_r\ln(S/S_0), \tag{14}$$

where S is the meter reading and S_0 is its value for $d=0$.

The experimental points plotted in Fig. 7 have been obtained using Eq. (14) and the theoretical curve, Eq. (7), has been calculated taking $n=1.26$. Again, the results are satisfactory. However, a more accurate analysis could be carried out to take into account the effects of using finite microwave beams.[15]

It should be pointed out that we were particularly interested in giving a simplified discussion of the experimental results, provided it is satisfactory. However, we have already mentioned the possibility of taking into account the finite size of the microwave beams, which would lead to a rather more complex theory. We should mention, as well, that we have neglected the effects of the walls of the prisms. Although they are relatively thin, their effects might be not negligible. If any student is interested in calculating the effects of the walls, we suggest using the standard matrix method for thin film multilayers.[16] Developing such a method might be useful, as well, if our experimental arrangement has to be used to simulate the one-dimensional motion of a particle through a set of potential barriers of different widths and heights.

V. CONCLUSIONS

A set of microwave experiments suitable for an educational laboratory has been described, enabling one to investigate accurately the characteristics of electromagnetic evanescent waves and tunneling effects. The use of microwaves instead of light reduces the mechanical accuracy requirements and simplifies the setup. The proposed experimental arrangements can be used to simulate the one-dimensional motion of a particle in quantum mechanics.

ACKNOWLEDGMENTS

The authors are grateful to Dr. P. Gonzalez for his contributions to these experiments. F. A. and S. N. wish to thank the Club Rotary Valencia Centro for giving financial support to the open competition of Physics Experiments at the University of Valencia, Spain. The first prize was awarded in 1991 to the set of experiments described in this paper.

[1] R. G. Hunsperger, *Integrated Optics: Theory and Technology* (Springer-Verlag, New York, 1985).
[2] B. Culshaw and J. Dakin, *Optical Fiber Sensors: System and Applications (Vol. II)* (Artech House, Boston, 1989).
[3] R. Eisberg and R. Resnik, *Quantum Physics of Atoms, Molecules, Solids, Nuclei, and Particles* (Wiley, New York, 1974).
[4] J. H. Hinken, *Superconductor Electronics, Fundamentals and Microwave Applications* (Springer-Verlag, New York, 1989).
[5] G. Binning and H. Rohrer, "The scanning tunneling microscope," Sci. Am. **253** (2), 40–46 (1985).
[6] S. Zhu, A. W. Yu, D. Hawley, and R. Roy, "Frustrated total internal reflection: A demonstration and review," Am. J. Phys. **54**, 601–607 (1986).
[7] J. J. Brady, R. O. Brick, and M. D. Pearson, "Penetration of microwaves into the rarer medium in total reflection," J. Opt. Soc. Am. **50**, 1080–1084 (1960).
[8] D. D. Coon, "Counting photons in the optical barrier penetration experiment," Am. J. Phys. **34**, 240–243 (1966).
[9] C. W. Leming and A. Van Smith, "A numerical study of quantum barrier penetration in one dimension," Am. J. Phys. **59**, 441–443 (1991).
[10] J. R. Reitz, F. J. Milford, and R. W. Christy, *Foundations of Electromagnetic Theory* (Addison-Wesley, Reading, MA, 1979).
[11] E. Hecht and A. Zajac, *Optics* (Addison-Wesley, Reading, MA, 1974).
[12] P. F. Combes, J. Graftenil, and J. F. Santereau, *Microwave Components, Devices and Active Circuits* (Wiley, New York, 1987).
[13] J. Navasquillo, V. Such, and F. Pomer, "A general method for treating the incidence of a plane electromagnetic wave on a plane interface between dielectrics," Am. J. Phys. **57**, 1109–1112 (1989).
[14] K. Chu and J. D. Noble, "Microwave demonstration of the spatial shift due to the evanescent wave," Am. J. Phys. **59**, 477–478 (1991).
[15] F. Pomer and J. Navasquillo, "The fields of a bounded electromagnetic beam propagating through an air gap between two dielectrics for frustrated total reflection," Am. J. Phys. **58**, 763–768 (1990).
[16] H. A. Macleod, *Thin Film Optical Filters* (Adam Hilger, United Kingdom, 1986).